THE JOURNAL OF PHYSICAL CHEMISTRY C

Article

pubs.acs.org/JPCC

Magnetic Field Effects on the Current of PCPDTBT-based Diode

O. Taboubi,[†] M. Radaoui,[†,§] A. Ben Fredj,*[,†] S. Romdhane,[†,∥] M. C. Scharber,[‡] N. S. Sariciftci,[‡] and H. Bouchriha[†]

[†]Laboratoire Matériaux Avancés et Phénomènes Quantiques, Faculté des Sciences de Tunis, Université de Tunis El Manar, 2092 Campus Universitaire, Tunis 2092, Tunisia

[‡]Linz Institute for Organic Solar Cells (LIOS), Johannes Kepler University Linz, Altenbergerstr. 69, 4040 Linz, Austria

[§]Faculté des Sciences de Gafsa, Campus Universitaire Sidi Ahmed Zarroug, 2112 Gafsa, Tunisia

[∥]Faculté des Sciences de Bizerte, Université de Carthage, 7021 Zarzouna, Bizerte, Tunisia

ABSTRACT: We investigate the magnetic field effect on the current of a diode based on a copolymer, poly{[4,4-bis(2-ethylhexyl)-cyclopenta-(2,1-*b*;3,4-*b*′)dithiophen]-2,6-diyl-*alt*-(2,1,3-benzo-thiadiazole)24,7-diyl} (PCPDTBT), which is intensively used in bulk heterojunction solar cells. Magnetoconductance measurements are carried out for applied voltages corresponding to the trap-charge-limited current regime. An effective mobility is introduced to take into account the presence of traps. The magnetoconductance is positive and monotonic in the full range of the applied voltages. The stochastic Liouville equation is a useful tool to interpret the magnetic field effect on the current. The latter equation is adapted in the framework of the electron−hole pair model to reproduce the line shape of magnetoconductance. The recombination rates, deduced from the fitting of the experimental data, are $k_S \approx 10^9$ s^{-1} and $k_T \approx 10^5$ s^{-1} for singlet and triplet e−h pairs, respectively.

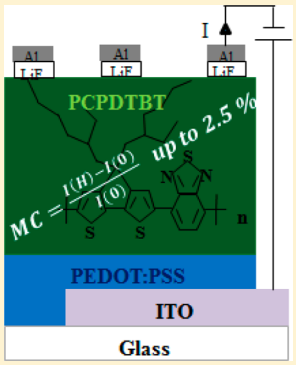

1. INTRODUCTION

Organic semiconductor (OSCs) materials are promising candidates that have a great deal of attention in the field of electronic and optoelectronic devices like organic light-emitting diodes (OLEDs), organic field-effect transistors (OFETs),[1,2] and organic photovoltaics (OPVs).[3−9] During these past decades, research on OSCs has attracted considerable attention owing to their potential advantages over their inorganic counterparts such as the facility of processing of the substrates, structural flexibility of the devices, and the low cost. A fascinating effect called organic magnetoresistance (OMR) has been observed by Francis et al.[10] at room temperature. A relatively small applied magnetic field of 10 mT can influence the conductance of OLEDs with nonmagnetic electrodes. This effect, which is defined as OMR = $\frac{I(0)-I(H)}{I(H)}$, where $I(H)$ and $I(0)$ are the currents in the presence and the absence of an applied magnetic field, respectively, could astonishingly reach 10%.[10]

Several explications have been proposed to probe the underlying mechanisms of the organic magnetoconductance (MC), which is expressed as MC = $\frac{I(H)-I(0)}{I(0)}$.[10−26] It was reported that depending on the operating conditions such as temperature,[12−14] applied voltage,[15−17] and orientation of the magnetic field with respect to the current flow,[18] the MC could be either positive or negative. The MC also depends on the organic material itself and its thickness.[19,20]

The study of these magnetic field effects provides a deep fundamental understanding of spin-physics and charge transport in OSCs. Several different models have been suggested as a potential explanation for the MC effect in literature. The bipolaron model proposed by Bobbert et al.[21] predicts that the effect can be seen in unipolar structures. In the case of electron and hole injection, two models were suggested. The electron−hole (e−h) pair model was proposed by Prigodin et al.,[22] who suggested that the charge transport in OSCs is limited by the e−h recombination. Hu et al.[24] suggested that both e−h pairs and excitons can contribute to the generation of secondary charge carriers (electrons and holes) through two channels: dissociation and charge reaction. Desai et al.[23] suggested that in OLEDs scattering between free carriers and triplet excitons results in a decrease in the carrier mobility. By applying a magnetic field the efficiency of the device is increased due to triplet to singlet conversion. Meanwhile, magnetic fields have shown large effects on other fields such as GMR sensors[26−30] and magnetic-field-induced capacitance enhancement.[31,32]

By analyzing the experimental data from different groups, it is summarized that the line shape of MC can be fitted either by Lorentz or by non-Lorentz formula, $\frac{B^2}{(B^2+B_0^2)}$ or $\frac{B^2}{(B_0+|B|)^2}$, where B_0 is a fitting parameter whose value is hyperfine-related parameter,[16,33] or by resolving the stochastic Liouville equation in the framework of an electron−hole pair model or triplet−doublet quenching.[17,25] The poly{[4,4-bis(2-ethylhexyl)-cyclopenta-(2,1-*b*;3,4-*b*′) dithiophen]-2,6-diyl-*alt*-(2,1,3-benzo-

Received: April 14, 2017
Revised: May 10, 2017
Published: May 10, 2017

DOI: 10.1021/acs.jpcc.7b03539
J. Phys. Chem. C 2017, 121, 11727−11732

thiadiazole)24,7-diyl} (PCPDTBT), containing alternating electron-donor and electron-acceptor units with a small band gap ($E_g \approx 1.75$ eV),[3] has been used in solar cells. The synthesis of PCPDTBT was described elsewhere, and its structure was also given.[3,6] PCPDTBT is one of the most promising materials for its high performance in OPVs[4,6] and OLEDs.[8]

We report the MFEs on the current in an organic diode based on PCPDTBT at room temperature for different applied voltages. The range of the applied voltages, corresponds to the trap-charge-limited current (TCLC) regime. In this regime, the electron current is characterized by a much steeper voltage dependence compared with the hole current, accompanied by a strong thickness dependence. This behavior attributed to trap-limited conduction (TLC), with the electron traps distributed exponentially in the bandgap.[34] We introduce an effective mobility to take into consideration the presence of traps. We show that the MFEs on the current in the device can be explained in the framework of the e−h pair model using a stochastic Liouville equation.

2. EXPERIMENTAL METHOD

The PCPDTBT solution was prepared with concentration of 15 mg/mL. The ITO glass substrates are cleaned using deionized water, two successive baths for 15 min in an ultrasonic cleaner with acetone and isopropanol (50 °C), and blown dry using nitrogen. Then, the ITO was treated in oxygen plasma for 5 min at 50 W. Device preparation was performed under ambient conditions, except for the evaporation of the top electrode. First, the substrate was covered by spin coating a poly(3,4-ethylenedioxythiophene) poly(styrenesulfonate) PEDOT:PSS (Clevios P VP AI 4083) after filtration using a 5 μm filter at 2000 rpm for 30 s and then annealed at 110 °C on a hot plate for 10 min. Second, the deposition of the active layer was at 1000 rpm at 30 s. Next, the sample was moved into a glovebox with a nitrogen atmosphere in a high vacuum system. The device was finalized by the deposition of a 1 nm thick lithium fluoride (LiF) layer and an aluminum (Al) layer of ∼100 nm as top electrodes. LiF and Al were thermally evaporated under high vacuum $p \approx 10^{-6}$mbar.

The device, with the structure ITO/PEDOT:PSS/PCPDTBT/LiF/Al, was then encapsulated with a glass cover using a UV-curable epoxy sealant with a UV exposure time of 15 min (Figure 1a).

From Figure 1b, by the application of an external electric field, free carriers were injected into the active layer after crossing the barrier offered by the electrode/PCPDTBT interfaces. The injection barrier for anode/PCPDTBT was ∼0.15 eV and that for PCPDTBT/cathode was ∼0.1 eV. Because the mobility of these carriers was low, a space-charge region inside the device that limits the current flow was formed. The current is thus referred to as space-charge-limited current (SCLC).[35] Moreover the presence of trap state predicts the existence of trap-charge-limited current (TCLC) regime.[36,37]

The device was then placed between the poles of an electromagnet and measurements were performed in the dark under ambient conditions.

3. MAGNETIC FIELD EFFECT

3.1. Results. We plotted in Figure 2 the double logarithmic scale of J−V characteristics, that is, $\log(J) \propto m \log(V)$. A first glance reveals the existence of three distinct regions: $m = 1$ for the ohmic contact, $m = 2$ in the SCLC, and TCLC for $m \geq 3$.

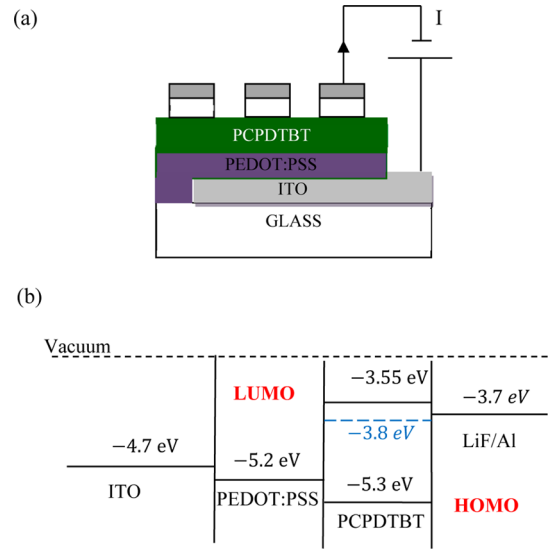

Figure 1. (a) Device structure: ITO/PEDOT:PSS/PCPDTBT/LiF/Al. (b) Schematic diagram of electronic levels of the device (the dotted blue line refers to the trap level).

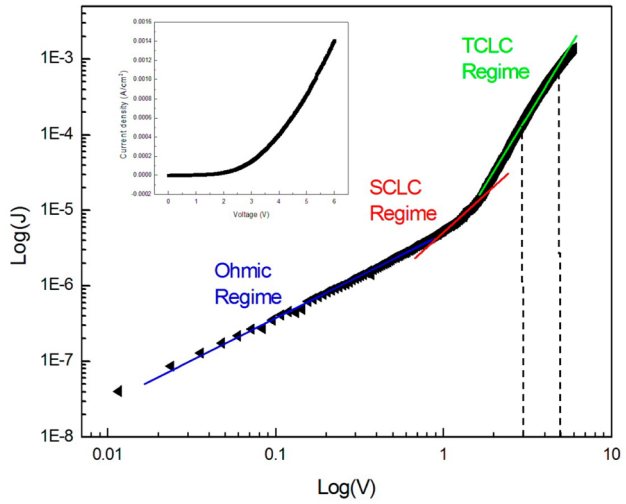

Figure 2. Current−voltage characteristic plotted on log−log scale. The inset shows the current as a function of the applied voltage.

In the TCLC regime the current density is approximated as[38]

$$J = e\mu N_H \left(\frac{\varepsilon_r \varepsilon_0 m}{N_t e(m+1)} \right)^m \left(\frac{2m+1}{m+1} \right)^{m+1} \frac{V^{m+1}}{d^{2m+1}} \quad (1)$$

where $m = \frac{E_t}{kT}$, E_t is the characteristic energy, kT is the energy characterizing the trap distribution, N_H is the effective density of states in the conduction band, $N_t \approx 4 \times 10^{23} m^{-3}$ is the total density of traps, V is the applied voltage across the semiconductor layer whose thickness is d, μ is the free-carrier mobility, ε_r is the relative dielectric constant of the organic layer, and ε_0 is the permittivity of vacuum.[38]

Furthermore, it is shown that using the Langevin recombination process is not sufficient to correctly describe the current−voltage behavior at low electric field; as a result, the total recombination rate coefficient is conferred by the expression: $B = (b_{SRH} + b_L)(np - n_i^2)$. b_{SRH} is the trap-assisted recombination first proposed by Shockley−Read−Hall (SRH)

DOI: 10.1021/acs.jpcc.7b03539
J. Phys. Chem. C 2017, 121, 11727−11732

and is expressed as $b_{SRH} = \frac{N_t C_n C_p}{C_n(n+n_1)+C_p(p+p_1)}$, *where* C_p and C_n are the capture coefficients for electrons and holes, respectively, n is the electron density in the conduction band and p is the hole density in the valence band, and n_i is the intrinsic carrier concentration in the sample. Under equilibrium conditions $p_1 n_1 = N_{cv} \exp\left(\frac{-E_{gap}}{k_B T}\right) = n_i^2$, where N_{cv} is the effective density of states, T is the temperature, and k_B is the Boltzmann constant. An approximation is submitted that when the hole mobility is more important than the electron mobility, thus $C_p \ll C_n$, the trap-assisted recombination is assimilated to $b_{SRH} = C_p N_t p$ with $C_p = \frac{q}{\epsilon}\mu_h$.[36,37,39] The Langevin recombination coefficient is expressed as $b_L = \frac{e}{\epsilon_r \epsilon_0}(\mu_e + \mu_h)$.

To calculate the hole (electron) mobility, Morana and coworkers studied the charge-carrier injection in PCPDTBT OTFT using Au as source and drain metal, and they used a low work function metal electrode LiF/Al to reduce the energetic barrier between the electrode and the HOMO (LUMO) of the polymer. The electron mobility was found to be $\mu_e = 3 \times 10^{-5}$ $cm^2\ V^{-1}\ s^{-1}$, two orders of magnitude lower than the hole mobility $\mu_h = 10^{-3}$ $cm^2\ V^{-1}\ s^{-1}$.[9]

Furthermore, Nicolai et al.[36] have shown that for PCPDTBT polymer the LUMO level is about −3.55 eV and the trap distribution level is at −3.8 eV. As a result, the trap states are considered to participate in the charge transport.[27] Hence we have used in our modeling an effective mobility $\mu_{eff} = \theta_{eff}\mu_0$, where[40,41]

- $\theta_{eff} = \frac{N}{N_t + N} \approx 0.2$, where N_t and N are the trapped and mobile charge carrier densities, respectively.
- $\mu_0 = \sqrt{\frac{\mu_e \mu_h (\mu_e + \mu_h)}{\mu_{rec}}}$ is the charge mobility in the SCLC, where $\mu_{rec} = \frac{\varepsilon B P_r}{2e}$ is the recombination mobility and P_r is the recombination probability of an electron−hole pair depending on the density matrix.[15,17]

By replacing $m = 2$ in eq 1, the current density is expressed as

$$J = 2\mu_{eff}\left(\frac{\epsilon_r \epsilon_0}{N_t}\right)^2 \frac{N_H}{e}\frac{V^3}{d^5} \tag{2}$$

As a result, the current density is inversely proportional to the square root of the recombination probability, $\alpha \frac{1}{\sqrt{P_r}}$. The latter expression was used to theoretically study the line shape of MC.

Figure 3 shows the MC as a function of the magnetic field for different applied voltages at room temperature. The MFE was strictly positive and monotonic in the full range of the applied voltages. The MFE saturates at 50 mT and decreases, from 2.5% (at 3 V) to 0.8% (at 5.25 V), by increasing the applied voltage. In addition, the red solid lines represent the theoretical investigation, which is obtained by resolving eq 3.

3.2. Discussion. In organic diodes, electrons and holes are injected into the device, and we know that random electron and hole capture generates four e−h pair states with 25% fraction for singlet state and 75% fraction for the three triplet states $(e-h)^3_{m=1,0,-1}$ based on spin statistics. These e−h pairs can recombine into singlet (S) and triplet (T) excitons with rates k_S and k_T and dissociate with rates q_S and q_T for singlet and triplet e−h pairs, respectively.

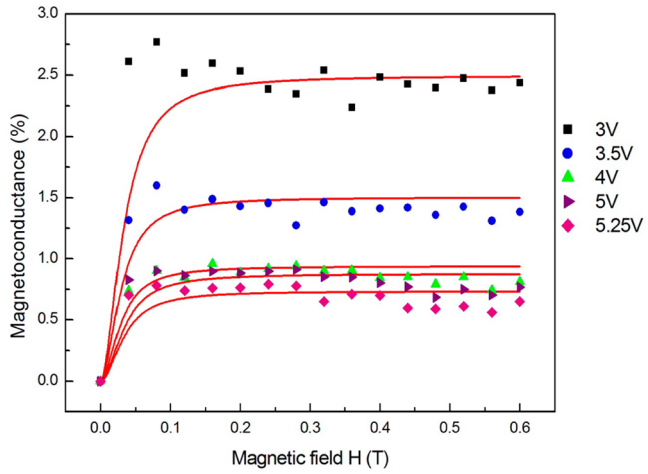

Figure 3. Magnetoconductance (MC) as a function of the applied magnetic field at forward bias voltages at room temperature. The red solid lines refer to the theoretical calculations.

On the basis of the electron−hole (e−h) pair model, proposed by Prigodin et al.,[22] we assume that e−h pairs in singlet state have a larger recombination rate k_S and thus a larger recombination probability.[22]

In the absence of magnetic field, the hyperfine fields experienced by the electron and the hole in the e−h pair state mix the singlet and triplet spin states (T_{+1}, T_0, T_{-1}). By applying a magnetic field, the mixing by the hyperfine fields is reduced through removing the spin degeneracy of triplet substates of e−h pairs. By increasing the magnetic field, the number of pair states being mixed with the singlet state decreases, leading to a decrease in the recombination of singlet e−h pairs and as a result an increase in the current.

To interpret the MFE, we used a stochastic Liouville equation (SLE) in the framework of the electron−hole (e−h) pair model. Under the steady-state condition the SLE is expressed by[17]

$$0 = -\frac{i}{\hbar}[H, \rho] - \frac{1}{2}(q_S + k_S)\{\Lambda_S, \rho\} - \frac{1}{2}(q_T + k_T)\{\Lambda_T, \rho\} + \Gamma \tag{3}$$

where H is the Hamiltonian of the system that is supposed to be the sum of Zeeman Hamiltonian $H_{Z,i} = g\mu_B \vec{H}_{app}.\vec{S}_i$ and Hyperfine Hamiltonian $H_{hf,i} = g\mu_B \vec{H}_{hyp,i}.\vec{S}_i$, where $g \approx 2$ is the polaron g factor, μ_B is the Bohr magneton, $\vec{H}_{app}$ is the applied magnetic field, $\vec{H}_{hyp,i}$ is the hyperfine field, and $\vec{S}_i$ is the spin operator of the individual polarons, where i denotes the hole or the electron.

k_S and k_T are recombination rates to an excitonic state from (e−h) pair state; q_S and q_T the dissociation rates of e−h pair to free charge carriers, Λ_S and Λ_T are the projection operators onto the singlet and triplet e−h pair states, respectively, and Γ is the identity matrix corresponding to the creation of spin pairs.

By resolving eq 3 under steady-state conditions, we obtained the e−h pair density matrix elements. Therefore, the recombination probability (P_r) is given by[17,25]

$$P_r = \frac{k_S \rho_{1,1} + \sum_{n=2}^{n=4} k_T \rho_{n,n}}{(k_S + q_S)\rho_{1,1} + \sum_{n=2}^{n=4}(k_T + q_T)\rho_{n,n}} \tag{4}$$

DOI: 10.1021/acs.jpcc.7b03539
J. Phys. Chem. C 2017, 121, 11727−11732

where $n = 1$ refers to the singlet and $n = 2$, 3, and 4 refers to the triplets.

The MC expression used in our theoretical study as a function of the recombination probability (P_r) is

$$MC = \frac{P_r(H)^{-\frac{1}{2}} - P_r(0)^{-\frac{1}{2}}}{P_r(0)^{-\frac{1}{2}}} \quad (5)$$

where $P_r(H)$ and $P_r(0)$ are the recombination probabilities in the presence and in the absence of magnetic field, respectively.

In Figure 3, we present the best agreement between the experimental results and the theoretical calculations using eq 5 and a hyperfine field $\sigma_{hf} \approx 1$ mT. The derived parameters are displayed in Table 1 (5% uncertainty).

Table 1. Fitting Parameters Used in the Theoretical Calculations

	parameters		
voltages (V)	k_S (10^9 s^{-1})	k_T (10^5 s^{-1})	$q_S = 2q_T$ (10^4 s^{-1})
3	5.5	2.2	5.5
3.5	6	3.5	6
4	7	5.3	7
5	9	6	9
5.25	9.3	6.8	9.3

From Table 1, we note that the recombination of e−h pairs is a dominant process as compared with the dissociation one; that is, k_S and k_T are greater than q_S and q_T. In addition, $k_S > k_T$, which confirms the hypothesis that e−h pairs in the singlet state have a larger recombination rate.

Moreover, in our calculation we have assumed that $q_S = 2q_T$; that is, e−h pairs in singlet state have a larger dissociation rate in accordance with Hu et al.[24]

Figure 4 shows the recombination probability, P_r, versus the magnetic field, for different values of the applied voltage. As can

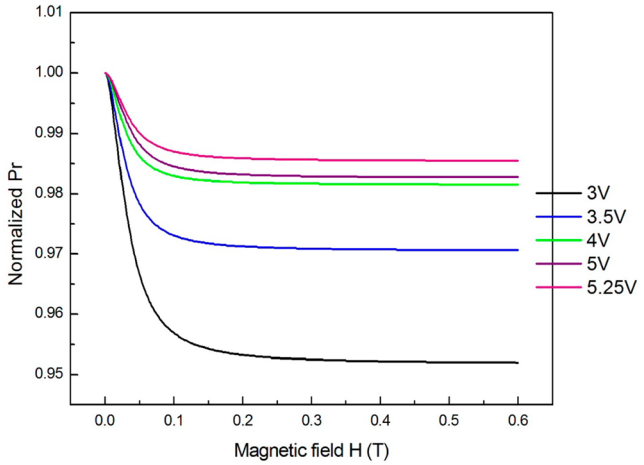

Figure 4. Normalized recombination probability as a function of the magnetic field at several applied voltages.

be seen, the recombination probability P_r decreases with increasing the magnetic field, which is in agreement with the boosting of the current and endorses the positive sign of the MC. Xu and Ma have shown that the current density decreases with increasing the recombination coefficient of e−h pairs in organic light-emitting diodes.[42] Furthermore, by increasing voltage, the recombination probability increases for all values of the magnetic field, leading to a decrease in the free charge carriers in the device and hence a decrease in the MFE on the current.

In addition, by increasing voltage more charge carriers are injected within the device, and thus the concentration of e−h pairs increases. However, only a small number of e−h pairs can serve as reaction centers for the MFE owing to the short e−h pair lifetime. In fact, by increasing the voltage the speed of the charge carriers increases, which leads to a decrease in e−h pair lifetime.[43] This result is consistent with the increase in the dissociation rates q_S and q_T.

4. CONCLUSIONS

Information technology is the basis of various industrial applications. Applications such as driverless cars and smart robots owe their existence to advances in manufacturing and the availability of sophisticated sensors.[44−46]

We performed a magnetic sensor based on the magnetoresistance effect in an organic semiconductor sandwich device. We studied the MFE on the current in a PCPDTBT-based diode for different applied voltages at room temperature. The MC effect reaches 2.5% in a magnetic field of 0.1 T and a 0.3 V applied voltage. To take into account the presence of traps we have introduced an effective mobility. Furthermore, we used an SLE in the framework of the e−h pair model to reproduce the MC line shapes. It has been found that by increasing the applied voltage the MFE on the current is reduced. Moreover, the recombination and dissociation rates of the singlet and triplet e−h pairs increase with increasing voltage. The singlet and triplet exciton lifetimes can be estimated by $\frac{1}{k_S} \approx$ ns and $\frac{1}{k_T} \approx \mu$s, respectively.

AUTHOR INFORMATION

Corresponding Author

*E-mail: amel.benfredj@fst.utm.tn.

ORCID

A. Ben Fredj: 0000-0002-5336-7792

Notes

The authors declare no competing financial interest.

ACKNOWLEDGMENTS

We gratefully acknowledge the financial support from the Ministry of High Education and Scientific Research of Tunisia and from Austrian Science Foundation FWF, within the project of Wittgenste in Prize for Prof. Sariciftci.

REFERENCES

(1) Sirringhaus, H. 25th Anniversary Article: Organic Field-Effect Transistors: The Path Beyond Amorphous Silicon. *Adv. Mater.* **2014**, *26*, 1319−1335.

(2) Dimitrakopoulos, C. D.; Malenfant, P. R. L. Organic Thin Film Transistors for Large Area Electronics. *Adv. Mater.* **2002**, *14*, 99.

(3) Zhu, Z.; Waller, D.; Gaudiana, R.; Morana, M.; Muhlbacher, D.; Scharber, M.; Brabec, C. Panchromatic Conjugated Polymers Containing Alternating Donor/Acceptor Units for Photovoltaic Applications. *Macromolecules* **2007**, *40*, 1981−1986.

(4) Scharber, M. C.; Koppe, M. J.; Cordella, G. F.; Loi, M. A.; Denk, P.; Morana, M.; Egelhaaf, H. J.; Forberich, K.; Dennler, G.; Gaudiana, R.; et al. Influence of The Bridging Atom on The Performance of a Low-Bandgap Bulk Heterojunction Solar Cell. *Adv. Mater.* **2010**, *22*, 367−370.

DOI: 10.1021/acs.jpcc.7b03539
J. Phys. Chem. C 2017, 121, 11727−11732

(5) Lee, J. K.; Ma, W. L.; Brabec, C. J.; Yuen, J.; Moon, J. S.; Kim, J. Y.; Lee, K.; Bazan, G. C.; Heeger, A. J. Processing Additives for Improved Efficiency from Bulk Heterojunction Solar Cells. *J. Am. Chem. Soc.* **2008**, *130*, 3619.
(6) Peet, J.; Kim, J. Y.; Coates, N. E.; MA, W. L.; Moses, D.; Heeger, A. J.; Bazan, G. C. Efficiency Enhancement in Low-Bandgap Polymer Solar Cells by Processing with Alkane Dithiols. *Nat. Mater.* **2007**, *6*, 497.
(7) Heeger, A. J. 25th anniversary article: Bulk Heterojunction Solar Cells: Understanding the Mechanism of Operation. *Adv. Mater.* **2014**, *26*, 10.
(8) Vandewal, K.; Tvingstedt, K.; Gadisa, A.; Inganäs, O.; Manca, J. V. On the Origin of The Open-Circuit Voltage of Polymer−Fullerene Solar Cells. *Nat. Mater.* **2009**, *8*, 904.
(9) Morana, M.; Wegscheider, M.; Bonanni, A.; Kopidakis, N.; Shaheen, S.; Scharber, M.; Zhu, Z.; Waller, D.; Gaudiana, R.; Brabec, C. Bipolar Charge Transport in PCPDTBT-PCBM Bulk-Heterojunctions for Photovoltaic Applications. *Adv. Funct. Mater.* **2008**, *18*, 1757−1766.
(10) Francis, T. L.; Mermer, O.; Veeraraghavan, G.; Wohlgenannt, M. Large Magnetoresistance at Room Temperature in Semiconducting Polymer Sandwich Devices. *New J. Phys.* **2004**, *6*, 185.
(11) Bloom, F. L.; Wagemans, W.; Kemerink, M.; Koopmans, B. Separating Positive and Negative Magnetoresistance in Organic Semiconductor Devices. *Phys. Rev. Lett.* **2007**, *99*, 257201.
(12) Liu, R.; Zhang, Y.; Lei, Y. L.; Chen, P.; Xiong, Z. H. Magnetic Field Dependent Triplet-Triplet Annihilation in Alq3-Based Organic Light Emitting Diodes at Different Temperatures. *J. Appl. Phys.* **2009**, *105* (9), 093719.
(13) Bloom, F. L.; Wagemans, W.; Koopmans, B. Temperature Dependent Sign Change of the Organic Magnetoresistance Effect. *J. Appl. Phys.* **2008**, *103*, 07F320.
(14) Zhang, Y.; Liu, R.; Lei, Y. L.; Xiong, Z. H. Low Temperature Magnetic Field Effects in Alq3-Based Organic Light Emitting Diodes. *Appl. Phys. Lett.* **2009**, *94*, 083307.
(15) Bergeson, J. D.; Prigodin, V. N.; Lincoln, D. M.; Epstein, A. J. Inversion of Magnetoresistance in Organic Semiconductors. *Phys. Rev. Lett.* **2008**, *100*, 067201.
(16) Mermer, Ö.; Veeraraghavan, G.; Francis, T.; Sheng, Y.; Nguyen, D.; Wohlgenannt, M.; Kohler, A.; Al-Suti, M.; Khan, M. Large Magnetoresistance in Nonmagnetic π-Conjugated Semiconductor Thin Film Devices. *Phys. Rev. B: Condens. Matter Mater. Phys.* **2005**, *72*, 205202.
(17) Radaoui, M.; Saidani, M. A.; Ben Fredj, A.; Romdhane, S.; Havlicek, M.; Egbe, D. A. M.; Sariciftci, N. S.; Bouchriha, H. Role of Recombination, Dissociation, and Competition Between Exciton-Charge Reactions in Magnetoconductance of Polymeric Semiconductor Device. *J. Appl. Phys.* **2014**, *116*, 183901.
(18) Cox, M.; Zhu, F.; Veerhoek, J. M.; Koopmans, B. Anisotropic Magnetoconductance in Polymer Thin Films. *Phys. Rev. B: Condens. Matter Mater. Phys.* **2014**, *89*, 195204.
(19) Gillin, W. P.; Zhang, S.; Rolfe, N. J.; Desai, P.; Shakya, P.; Drew, A. J.; Kreouzis, T. Determining the Influence of Excited States on Current Transport in Organic Light Emitting Diodes using Magnetic Field Perturbation. *Phys. Rev. B: Condens. Matter Mater. Phys.* **2010**, *82*, 195208.
(20) Taboubi, O.; Radaoui, M.; Ben Fredj, A.; Romdhane, S.; Egbe, D. A. M.; Bouchriha, H. Thickness Dependence of Organic Magnetoconductance of Polymeric Semiconductor Device Based on an Ambipolar Polymer AnE-PVstat. *Synth. Met.* **2017**, *227*, 117−121.
(21) Bobbert, P. A.; Nguyen, T. D.; Van Oost, F. W. A.; Koopmans, B.; Wohlgenannt, M. Bipolaron Mechanism for Organic Magnetoresistance. *Phys. Rev. Lett.* **2007**, *99*, 216801.
(22) Prigodin, V.; Bergeson, J.; Lincoln, D.; Epstein, A. Anomalous Room Temperature Magnetoresistance in Organic Semiconductors. *Synth. Met.* **2006**, *156*, 757.
(23) Desai, P.; Shakya, P.; Kreouzis, T.; Gillin, W. P. The Role of Magnetic Fields on the Transport and Efficiency of Aluminum tris(8-hydroxyquinoline) Based Organic Light Emitting Diodes. *J. Appl. Phys.* **2007**, *102*, 073710.
(24) Hu, B.; Wu, Y. Tuning Magnetoresistance Between Positive and Negative values in Organic Semiconductors. *Nat. Mater.* **2007**, *6*, 985.
(25) Schellekens, A. J.; Wagemans, W.; Kersten, S. P.; Bobbert, P. A.; Koopmans, B. Microscopic Modeling of Magnetic-field Effects on Charge Transport in Organic Semiconductors. *Phys. Rev. B: Condens. Matter Mater. Phys.* **2011**, *84*, 075204.
(26) Yan, X.; Gu, J.; Zheng, G.; Guo, J.; Galaska, A. M.; Yu, J.; Khan, M. A.; Sun, L.; Young, D. P.; Zhang, Q.; et al. Lowly Loaded Carbon Nanotubes Induced High Electrical Conductivity and Giant Magnetoresistance in Ethylene/1-octene Copolymers. *Polymer* **2016**, *103*, 315−327.
(27) Guo, J.; Guan, L.; Wei, H.; Khan, M. A.; Zhang, X.; Li, B.; Wang, Q.; Weeks, B. L.; Young, D. P.; Shen, T.; et al. Enhanced Negative Magnetoresistance with High Sensitivity of Polyaniline Interfaced with Nanotitania. *J. Electrochem. Soc.* **2016**, *163* (8), H664−H671.
(28) Bin, Q.; Qiu, B.; Guo, J.; Wang, Y.; Wei, X.; Wang, Q.; Sun, D.; Khan, M. A.; Young, D. P.; O'Connor, R.; et al. Dielectric Properties and Magnetoresistance Behavior of Polyaniline Coated Carbon Fabrics. *J. Mater. Chem. C* **2015**, *3*, 3989−3998.
(29) Gu, H.; Zhang, X.; Wei, H.; Huang, Y.; Wei, S.; Guo, Z. An Overview of The Magnetoresistance Phenomenon in Molecular Systems. *Chem. Soc. Rev.* **2013**, *42*, 5907.
(30) Wei, H.; Gu, H.; Guo, J.; Yan, X.; Liu, J.; Cao, D.; Wang, X.; Wei, S.; Guo, Z. Significantly Enhanced Energy Density of Magnetite/Polypyrrole Nanocomposite Capacitors at High Rates by Low Magnetic Fields. *Adv. Compos. Sci.* **2017**, in press.
(31) Zhu, J.; Chen, M.; Wei, H.; Yerra, N.; Haldolaarachchige, N.; Luo, Z.; Young, D. P.; Ho, T. C.; Wei, S.; Guo, Z. Magnetocapacitance Inmagnetic Microtubular Carbon Nanocomposites Under External Magnetic Field. *Nano Energy* **2014**, *6*, 180−192.
(32) Zhu, J.; Chen, M.; Qu, H.; Luo, Z.; Wu, S.; Colorado, H. A.; Wei, S.; Guo, Z. Magnetic Field Induced Capacitance Enhancement in Graphene and Magnetic Graphene Nanocomposites. *Energy Environ. Sci.* **2013**, *6*, 194−204.
(33) Wagemans, W.; Janssen, P.; Schellekens, A. J.; Bloom, F. L.; Bobbert, P. A.; Koopmans, B. The Many Faces of Organic Magnetoresistance. *SPIN* **2011**, *01*, 93−108.
(34) Mandoc, M. M.; de Boer, B.; Paasch, G.; Blom, P. W. M. Trap-Limited Electron Transport in Disordered Semiconducting Polymers. *Phys. Rev. B: Condens. Matter Mater. Phys.* **2007**, *75*, 193202.
(35) Moiz, S. A.; Ahmed, M. M.; Karimov, Kh. S; Rehman, F.; Lee, J. H. Space Charge Limited Current−voltage Characteristics of Organic Semiconductor Diode Fabricated at Various Gravity Conditions. *Synth. Met.* **2009**, *159*, 1336−1339.
(36) Nicolai, H. T.; Kuik, M.; Wetzelaer, G. A. H.; De Boer, B.; Campbell, C.; Risko, C.; Brédas, J. L.; Blom, P.W. M. Unification of Trap-Limited Electron Transport in Semiconducting Polymers. *Nat. Mater.* **2012**, *11*, 882.
(37) Kuik, M.; Wetzelaer, G.-J. A. H.; Nicolai, H. T.; Craciun, N. I.; De Leeuw, D. M.; Blom, P. W. M. 25th Anniversary Article: Charge Transport and Recombination in Polymer Light-Emitting Diodes. *Adv. Mater.* **2014**, *26*, 512−531.
(38) Kuik, M.; Koster, L. J. A.; Wetzelaer, G. A. H.; Blom, P.W. M. Trap-Assisted Recombination in Disordered Organic Semiconductors. *Phys. Rev. Lett.* **2011**, *107*, 256805.
(39) Brütting, W.; Berleb, S.; Mückl, A. G. Device Physics of Organic Light-Emitting Diodes Based on Molecular Materials. *Org. Electron.* **2001**, *2*, 1−36.
(40) Radaoui, M.; Hleli, E.; Ben Hamed, Z.; Ben Fredj, A.; Hrichi, H.; Romdhane, S.; Egbe, D. A. M.; Bouchriha, H. Spectroscopic Characterization of a Red Light-Emitting Polymer: Anthracene-Containing Poly(p-arylene-ethynylene)-alt-poly(p-arylene-vinylene). *Mater. Sci. Semicond. Process.* **2015**, *30*, 285−291.
(41) Juhasz, P.; Nevrela, J.; Micjan, M.; Novota, M.; Uhrik, J.; Stuchlikova, L.; Jakabovic, J.; Harmatha, L.; Weis, M. Charge Injection

DOI: 10.1021/acs.jpcc.7b03539
J. Phys. Chem. C 2017, 121, 11727−11732

and Transport Properties of an Organic Light-Emitting Diode. *Beilstein J. Nanotechnol.* **2016**, *7*, 47−52.
(42) Xu, K.; Ma, D. Electron−Hole Pair Model in Bulk-Limited Organic Light-Emitting Diodes. *J. Phys. Chem. C* **2015**, *119* (1), 640−643.
(43) Bagnich, S. A.; Niedermeier, U.; Melzer, C.; Sarfert, W.; von Seggern, H. Electron-Hole Pair Mechanism for The Magnetic Field Effect in Organic Light Emitting Diodes Based on poly(paraphenylene vinylene). *J. Appl. Phys.* **2009**, *106*, 113702.
(44) Alippi, C. A Unique Timely Moment for Embedding Intelligence in Applications. *CAAI Transactions on Intelligence Technology* **2016**, *1*, 1−3.
(45) Jin, H.; Chen, Q.; Chen, Z.; Hu, Y.; Zhang, J. Multi-LeapMotion Sensor Based Demonstration for Robotic Refine Tabletop Object Manipulation Task. *CAAI Transactions on Intelligence Technology* **2016**, *1*, 104−113.
(46) Zhang, X.; Gao, H.; Guo, M.; Li, G.; Liu, Y.; Li, D. A Study on Key Technologies of Unmanned Driving. *CAAI Transactions on Intelligence Technology* **2016**, *1*, 4−13.

DOI: 10.1021/acs.jpcc.7b03539
J. Phys. Chem. C 2017, 121, 11727−11732